Composite Structures 131 (2015) 17–24

Contents lists available at ScienceDirect

Composite Structures

journal homepage: www.elsevier.com/locate/compstruct

Dynamic and static characteristics of polypropylene pyramidal kagome structures

June-Sun Hwang [a], Tae-Gyun Choi [b], Dongyoung Lee [a], Min-Young Lyu [b], Dai Gil Lee [a], Dong-Yol Yang [a,*]

[a] School of Mechanical Aerospace & Systems Engineering, KAIST, 291 Daehak-ro, Yuseong-gu, Daejeon, Republic of Korea
[b] Department of Mechanical System Design Engineering, Seoul National University of Science and Technology, 232 Gongneung-ro, Nowon-gu, Seoul, Republic of Korea

ARTICLE INFO

Article history:
Available online 7 May 2015

Keywords:
Kagome structure
Composite sandwich
Three-point bending
Impact test

ABSTRACT

A sandwich structure is an effective light weighting construction to meet the increasing demand for lightweight engineered components. Generally, a truss-based kagome structure shows reinforced characteristics for bending compared with other truss-based sandwich structures. In this research, a pyramidal kagome structure, which is known as one of the most effective light weighting structures, was developed and fabricated with polypropylene using an injection molding process to reduce fabrication time and cost. Static and dynamic characteristics of the pyramidal kagome structure were investigated by three-point bending and drop weight impact tests. The results were compared with a conventional honeycomb structure. The developed pyramidal kagome structure showed similar specific bending stiffness and maximum bending load while impact load reducing capability was three times higher compared to the honeycomb structure. The results demonstrated the effectiveness of the newly developed pyramidal kagome structure.

1. Introduction

The manufacturing of lightweight structures is incoming more important in fields of engineering, especially in the aircraft or automobile industries. Sandwich structures, composed of inner core structures and outer face sheets, can reduce the weight of components, and can be the solution to material resource and energy problems [1,2]. Even though most of the inner core structure contains very little material, the remaining inner structure can effectively support an external load. Generally this kind of sandwich structure exhibits high specific strength.

The honeycomb structure, which is a typical closed cell structure, has been widely applied to the structural parts of airplanes because of its high specific strength and light weight characteristics [3]. Even though the honeycomb structure has good mechanical properties, it also has some disadvantages, such as in-plane shear mode weakness and difficultly when applied to a curved structure.

In the recent studies, truss-based open cell structures are considered as effective alternatives of the honeycomb structure [4–7]. The truss core sandwich can be adapted to the complex curved surfaces of the component [8] and the open cell cores can also absorb impact energy efficiently because of the elastic deformation of the inner struts [9]. The other advantage of the open cell structure is that the structure can be easily integrated with other functional properties, such as heat insulation material or soundproof material by inserting the functional materials inside the open cell structure [10,11].

The mechanical characteristics of open cell truss cores, such as the tetrahedral core [12,13], pyramidal core [14,15] and kagome core [16,17] have been extensively investigated. In previous studies, the sandwich structures were manufactured using metals because of their high mechanical strength. More recently, there have been attempts to replace metallic core structures with non-metallic materials such as polymers, or fiber reinforced plastics such as carbon fiber reinforced plastic (CFRP) or glass fiber reinforced plastic (GFRP).

Among various approaches, foam core based fiber reinforced composites have been manufactured using a Kevlar stitching method [18,19]. There have also been attempts to make a composite pyramidal truss-like structure by laser cutting or electrical discharge machining methods [20,21]. A micro scale truss structure was manufactured using photo curable polymer resin [22]. The manufacturing process for a hollow type CFRP composite structure was suggested by the thermal expansion molding method [23]. There have been some attempts to make a honeycomb structure composed of polymer core and fiber reinforced composite face

* Corresponding author. Tel.: +82 42 350 3214; fax: +82 42 350 5214.
E-mail address: dyyang@kaist.ac.kr (D.-Y. Yang).

http://dx.doi.org/10.1016/j.compstruct.2015.04.065
0263-8223/

sheets [24,25]. A kagome structure was fabricated by the wire woven method [26]. The kagome structure was superior in terms of mechanical properties compared to other truss structures, and in particular, the kagome structure showed excellent mechanical properties in compressive strength and buckling resistance [16]. However the manufacturing process of the woven kagome structure is complicated, even though a weaving machine was developed for this kind of woven wire kagome structure. The brazing process for welding kagome wires includes additional cost.

In this paper, a pyramidal kagome (PK) structure was developed based on the conventional kagome structure. The PK structure was fabricated by joining two pyramidal cores instead of woven wire method as shown in Fig. 1 to reduce the forming time and cost. The fabrication process of the PK structure was composed of three steps: manufacturing of a flat mesh by injection molding process, forming the pyramidal shape, and adhesion of two pyramidal structures. The material used for the PK structure was polypropylene (PP). The fabrication time was significantly reduced by employing the injection molding process. Furthermore, mechanical characteristics of the PK structure were examined by three-point bending and drop weight impact tests. The test results were compared with PP core based commercial honeycomb structure.

2. Manufacturing process of PK structure

The PK structure was fabricated by three steps. The processes involved the injection of the flat mesh, followed by forming of the pyramidal structure and joining of two formed pyramidal cores. The detailed procedures are introduced in detail as below. The shape parameters for fabrication are shown in Fig. 2. The height of the PK core is h, core strut angle is θ, the thickness of flat mesh is t, unit length of the pyramidal structure is l and the width of the strut is w.

Three different sizes of flat meshes were designed for parametric study of the PK structure. Those three flat meshes were designed to have the same height of 4.4 mm and strut width of 1.5 mm and the variable was strut angles which were 30°, 37.5°, 45°. The thickness of flat meshes was 0.4 mm, which was the minimum thickness that could be fabricated for flat mesh without defect by the injection molding process. The dimensions of PK structure are summarized in Table 1. The volume ratio is defined as the ratio of volume of each PK structure to same height of solid structure.

2.1. Flat mesh injection and fabrication of pyramidal structures

Mold for flat mesh injection molding was designed and manufactured as shown in Fig. 3(a). Three different sizes of flat meshes shown in Table 1 were made in one mold for PK structure by injection molding. Injection molding was conducted with 0.2 m/s of injection speed, 150 MPa of injection pressure, and an injection temperature of 290 °C. The injected material was PP (J-560S, Lotte chemical corp., South Korea) which has a melt index of 18 g/10 min. The injection molded flat mesh is shown in Fig. 3(b).

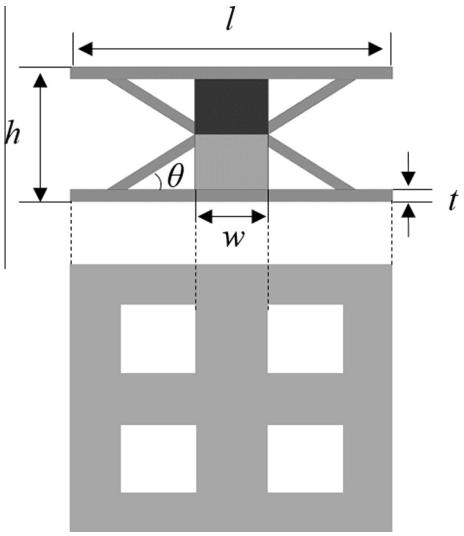

Fig. 2. PK structure and the shape parameters.

Table 1
Dimension of PK structures.

Core strut angle (°)	Thickness, t (mm)	Height, h (mm)	Width, w (mm)	Unit size, l (mm)	Volume ratio (%)	Flat mesh size (mm^2)
30	0.4	4.4	1.5	9.2	7.8	158.6 × 158.6
37.5	0.4	4.4	1.5	7.7	8.9	132.4 × 132.4
45	0.4	4.4	1.5	6.6	10.0	113.7 × 113.7

The flat meshes were formed into pyramidal structures by using upper and lower dies. The upper and lower dies were heated to 140 °C by cartridge heaters which were inserted to increase the flexibility of the PP meshes for forming. The forming load for the pyramidal structure was 300 N. The manufactured pyramidal structure is shown in Fig. 4.

2.2. Core joining process

The method of joining two pyramidal truss cores is important because debonding fracture by the external force can occur at the joining interface before the buckling of the core strut. Bonding of the polyolefin material such as polyethylene and polypropylene is difficult due to its nonpolar surface. To cope with the problem, surface treatment methods such as plasma treatment or corona treatment can be adopted to modify the nonpolar PP surface into a polar state [28]. In this study, an ultrasonic welding

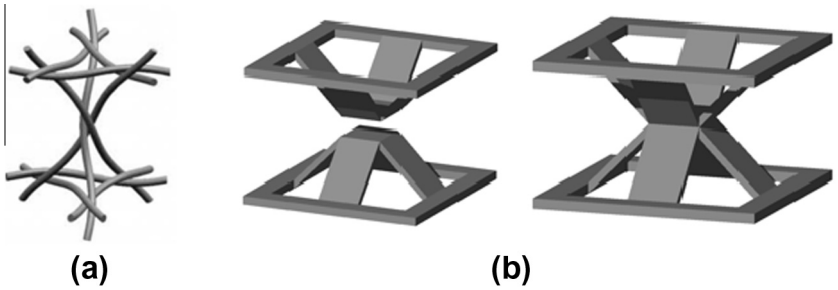

Fig. 1. Kagome structures: (a) woven kagome structure [27]; (b) PK structure.

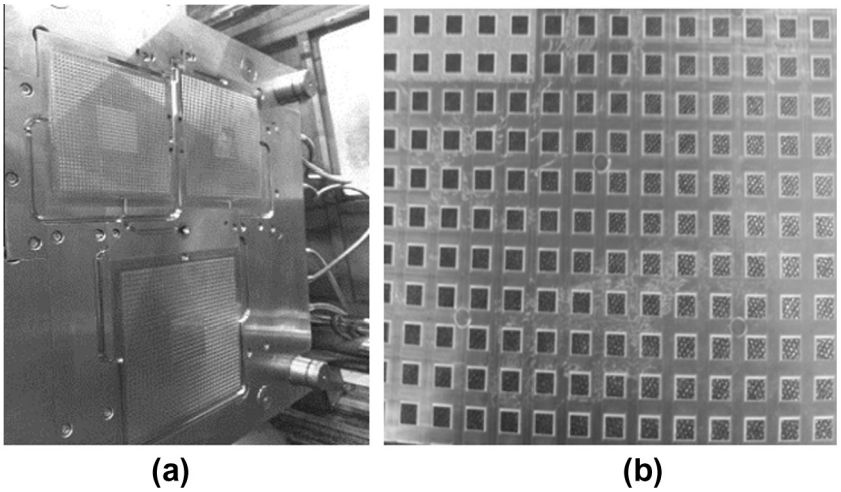

Fig. 3. Fabrication of the flat mesh: (a) mold for injection molding; (b) flat mesh for 45° core strut angle.

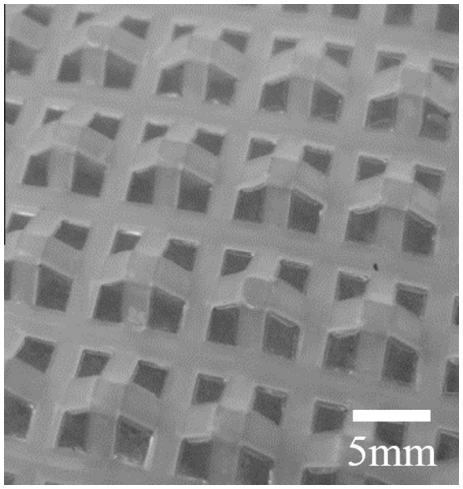

Fig. 4. Fabricated pyramidal truss core (45° core strut angle).

method was applied for joining. It is very fast, and the method guarantees high bonding strength between welded layers.

When ultrasonic welding was used, adhesion fracture was not observed. For the sample, the maximum shear stress of the welding interfaces above the tensile stress of the PP during single lap shear test, so necking occurred between the adhesion point and the fixed point at the jig. Based on these results, a 200 W grade ultrasonic welding device was made for bonding of pyramidal cores as shown in Fig. 5. The horn tip width of the welding tool was 1.5×1.5 mm^2.

2.3. Fabrication of sandwich structure for three-point bending and impact test

The structural characteristics of the PK sandwich structure were tested by three-point bending and impact tests. The flexural rigidity and capability to reduce the impact load of the PK sandwich structure was compared with a honeycomb sandwich structure made of PP. The honeycomb was composed of short pipe structures instead of conventional hexagonal structures as shown in Fig. 6. Each pipe was bonded by adhesive. The inner radius of the pipe structure was 8 mm and the wall thickness of the pipe was 0.4 mm.

As a face sheet, 0.4 mm thickness of GFRP plate was used to increase the structural strength of both honeycomb and PK structures, because the mechanical strength of the sandwich structure depends largely on the face sheets. The GFRP face sheet was plain weave glass fibers impregnated with epoxy resin. These GFRP face sheets were bonded to the upper and lower sides of the PK structure and the honeycomb structure by adhesive (AXIA 1500, AXIA, South Korea). Both face sheet and inner core was treated by primer (AXIA 1501, AXIA, South Korea), and dried for 30 min and then the

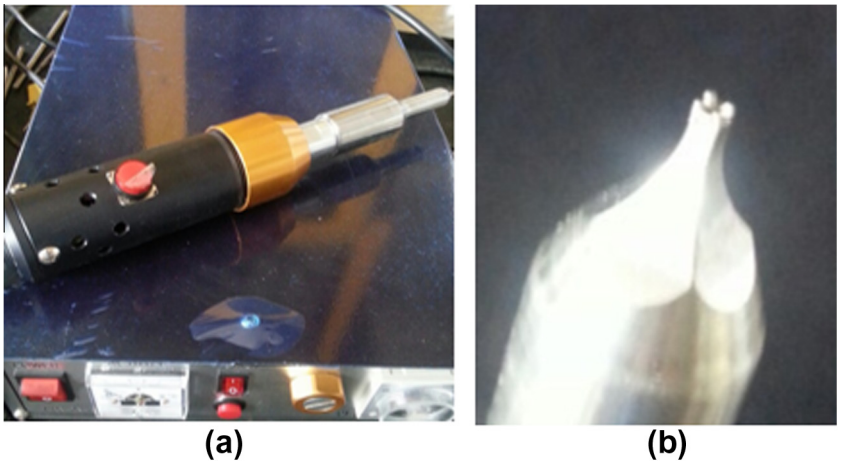

Fig. 5. Welding device: (a) ultrasonic wave welding device; (b) horn and tip.

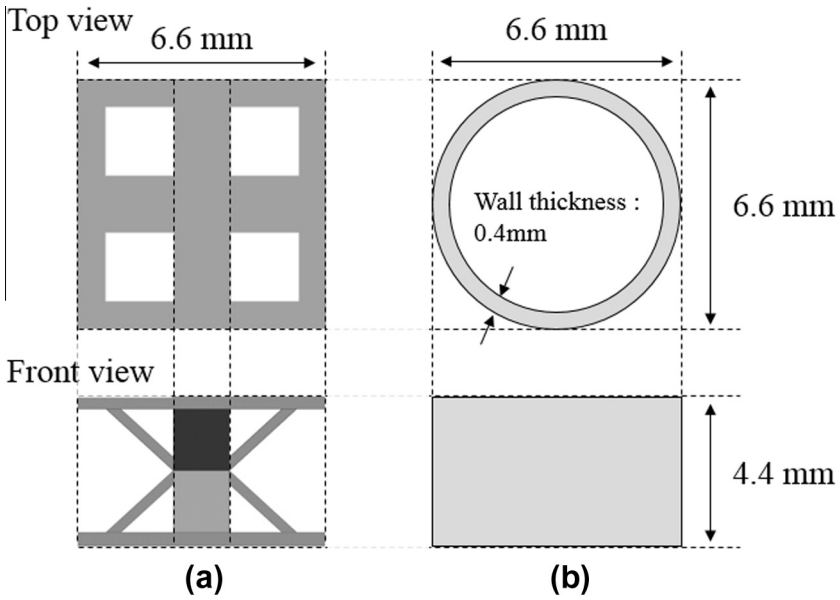

Fig. 6. Structural comparison: (a) PK; (b) pipe type honeycomb structure.

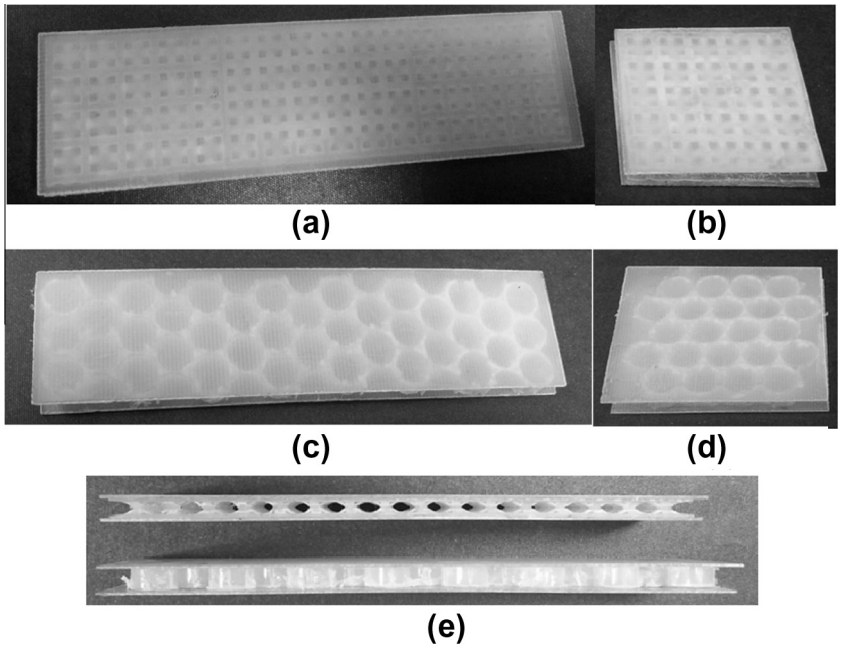

Fig. 7. Fabricated specimen: (a) 45° core strut angle PK sandwich structure for bending test; (b) 45° core strut angle PK sandwich structure for impact test; (c) honeycomb sandwich structure for bending test; (d) honeycomb sandwich structure for impact test; (e) front side of PK (upper) and honeycomb (lower) sandwich structure.

adhesive was applied and cured at room temperature for 24 h. The fabricated specimens are shown in Fig. 7 whose dimensions are indicated in Tables 2 and 3.

The material properties of PP and GFRP were obtained by material tests. Young's modulus of the PP was 1.2 GPa, Poisson's ratio was 0.35, yield strength of the polypropylene was 15 MPa. Young's modulus of the GFRP was 30 GPa and Poisson's ratio was 0.34.

3. Experimental set up

3.1. Three-point bending test

The three-point bending tests were conducted by using material testing machine (INSTRON 5583, Instron, USA). The radii of the nose and supports were 4 mm and the span length was 75 mm as shown in Fig. 8. The cross head speed was 2 mm/min.

3.2. Impact test

The impact tests were conducted with respect to the impact energy. The impact energy was calculated by controlling the height of the impactor. The impact energies were set to 1 J, 2 J, 3 J, 4 J, 5 J, and 6 J. The experimental set up is shown in Fig. 9. A cylindrical impact tup was used with the diameter of 70 mm. The weight of the impactor assembly was 1 kg. The impact loads were measured by a ring type force transducer (charge output force sensor 214B, PCB Piezotronics, USA) which was installed on the impact tup. All the specimens were fixed at the base by adhesive during the

Table 2
Dimensions of three-point bending test specimens.

Structure	Overall length (mm)	Overall height (mm)	Width (mm)
30° PK	111	5.2	28
37.5° PK	107	5.2	24
45° PK	105	5.2	22
Honeycomb	110	5.3	25

Table 3
Dimensions of drop weight impact test specimens.

Structure	Overall length (mm)	Overall height (mm)	Width (mm)
30° PK	38.5	5.2	38.5
37.5° PK	40	5.2	40
45° PK	41	5.2	41
Honeycomb	43	5.3	38

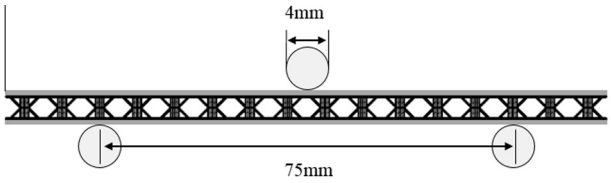

Fig. 8. Experimental set up for three-point bending test.

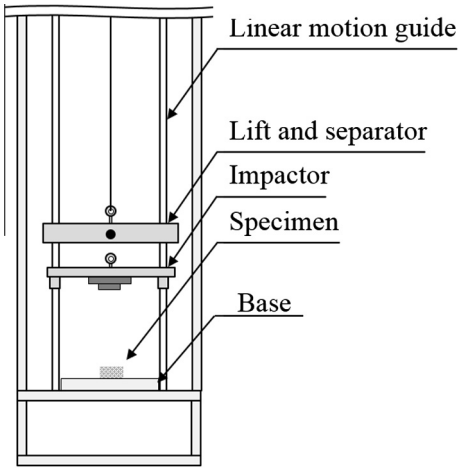

Fig. 9. Equipment for impact test [29].

impact test. The impact test was conducted three times for each test condition.

4. Discussion

4.1. Three-point bending test

The three-point bending tests were conducted to investigate structural stiffness and strength. Three different PK sandwich structures and the honeycomb sandwich structure were tested, and the results are shown in Fig. 10. The bending loads from the test were divided by the mass of each structure to calculate specific bending load. The 45° core strut angle PK (45° PK) sandwich structure showed the maximum bending load. This 45° PK sandwich structure was stably bent to 10 mm of deflection without any damages, while the honeycomb sandwich structure was fractured at

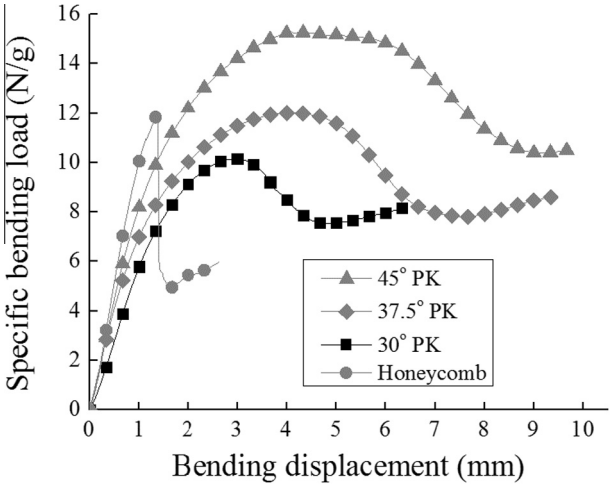

Fig. 10. Specific bending load–displacement curves of three-point bending experiments.

the adhesive interface at 1.2 mm of deflection. The maximum specific bending load of the 45° PK sandwich structure was 31% higher than that of the honeycomb sandwich structure. No adhesion failure was observed in any of the PK sandwich structures. The adherend between the face sheet and the core also remained undamaged. The specific bending stiffness of the 45° PK sandwich structure was 8.6 N/g·mm and the 37.5° PK, 30° PK, honeycomb sandwich structures were 7.5 N/g·mm, 5.9 N/g mm, and 10.4 N/g·mm, respectively. Even though the honeycomb sandwich structure showed the highest bending stiffness, it is difficult to be used as the structural part because the bending deformation was too limited. It means that the honeycomb structure could be fractured even with small bending deformation when adopted as the structural component.

There were two reasons why the adherend fracture of honeycomb sandwich structure occurred. First is that the adherend area of the PK sandwich structure is 2.8 times bigger than that of the honeycomb sandwich structure because of its structural characteristic. The other reason is the buckling resistance of the honeycomb core. Bending of the sandwich structure should accompany shear deformation toward longitudinal direction, as shown in Fig. 11. However, shear deformation in the honeycomb structure was hard because of its high buckling resistance, and this characteristic resulted in the interfacial failure of the honeycomb sandwich structure.

However, shear deformation of a honeycomb structure was limited, as shown in Fig. 12(a). The shear stress did not reach the level of buckling stress of the honeycomb structure in this experiment, while shear stress increased over the critical shear strength of the adhesive. When the shear stress reached the shear strength of the adhesive, the honeycomb core and face sheet were debonded as shown in Fig. 12(b). The upper face sheet protruded to the left side because of the adhesive failure. For these reasons, the adherend fracture of honeycomb sandwich structure occurred at the small deflection.

4.2. Investigation of shear stress at adherend area

Shear stress at the adhesive interface reached the critical value of the adhesive before the honeycomb core buckled. However, adhesion failure can occur as a result of poor adhesion conditions produced during fabrication of specimen. For this reason, the shear stress value of the adherend was examined in this research. The shear stress between adhesion interfaces was calculated by using

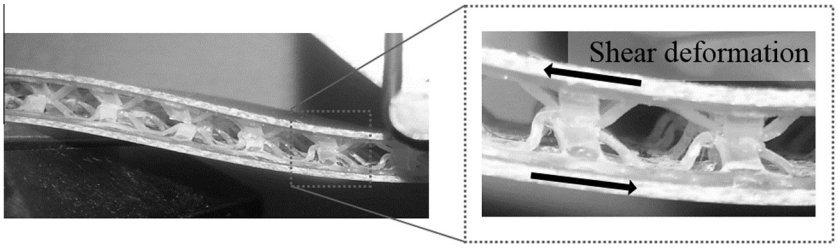

Fig. 11. Bending of the PK sandwich structure.

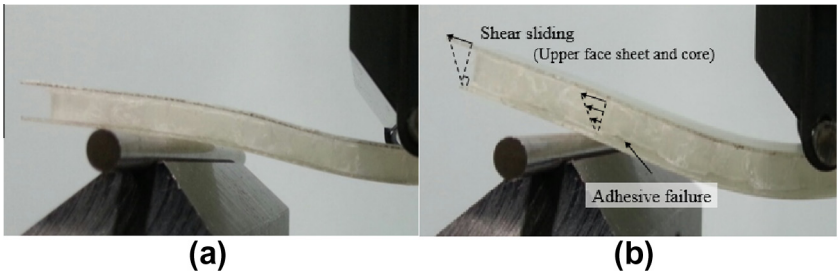

Fig. 12. Bending deformation of honeycomb sandwich structure: (a) before debonding; (b) after debonding.

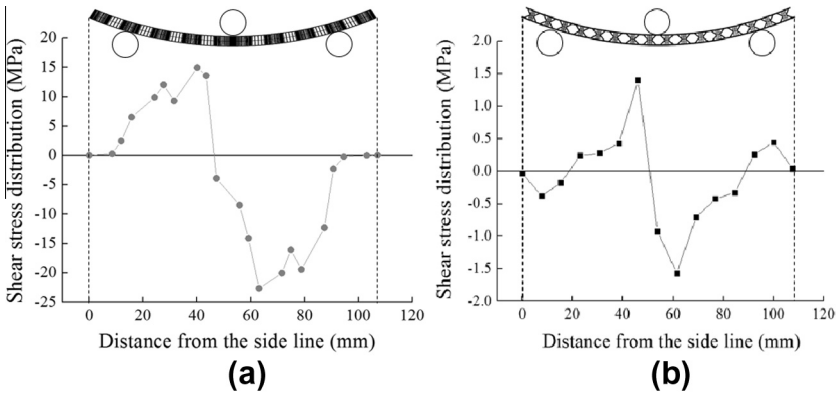

Fig. 13. Shear stress distribution at the adherend along the longitudinal direction at 10 mm deflection: (a) honeycomb sandwich structure; (b) PK sandwich structure.

the commercial finite element analysis software (ABAQUS, Dassault systems, France). The analysis was conducted with the 45° PK sandwich structure and honeycomb sandwich structure to compare the structural differences. The face sheet meshes were made to have three elements in the thickness direction. The numbers of meshes for the PK sandwich structure and the honeycomb sandwich structure were 59,392 and 24,288, respectively. The core material and surface sheets were assumed to be in a perfectly bonded state during the bending analysis.

Even though the assumption of perfect bonding was an unrealistic assumption, the measured shear stress of the adhesive interfaces can be used to evaluate when the shear stress of the adhesion interfaces reached the critical shear stress of 4 MPa which was the value obtained from single lap shear test. The shear stress distribution was calculated at the adherend after 10 mm of deflection, and the result is shown in Fig. 13. The maximum shear stress was observed at points of 45 mm and 60 mm from the left end of the PK specimen. This tendency of shear stress distribution was the same in the case of the honeycomb sandwich structure. The peak load also appeared at points 10 mm from the center of the honeycomb sandwich structure as shown in Fig. 13(b).

Those two points were expected to undergo failure during the bending experiment. Therefore, the shear stress history was measured at two expected points as shown in Fig. 14. The shear stress at the adherend of the honeycomb sandwich structure exceeded the shear strength at 1.1 mm of deflection. This indicates that adhesive failure would occur after 1.1 mm of deflection, which was very similar to the experimental result. The shear stress did not exceed the critical shear strength of adhesive in the case of the PK sandwich structure, and this result explains why the adhesive failure did not occur in the PK sandwich structure bending experiment.

4.3. Impact test

The impact test was conducted to examine the ability of the structures to reduce the maximum impact load. The peak impact load measured at the impactor is shown in Fig. 15. The 30° PK sandwich structure was considered to be the most effective design for low impact energy levels, such as 1 J and 2 J. However, the impact load reduction of the 30° PK sandwich structure became inefficient with increasing impact energy above 3 J because the pyramidal core was fully compressed and additional deformation was limited above 3. Three PK sandwich structures were more effective than the honeycomb sandwich structure within the impact energy levels of interest. The impact load reduction of the

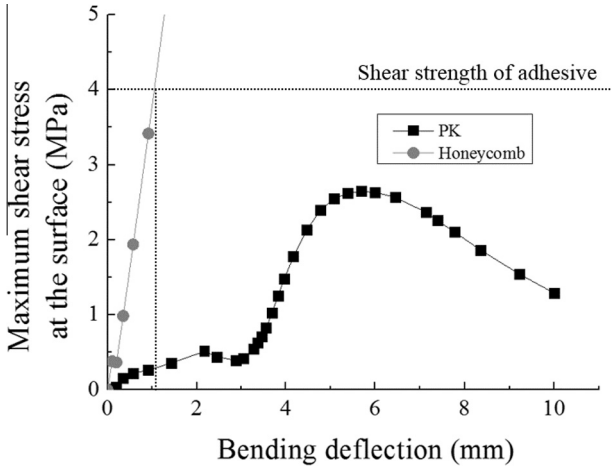

Fig. 14. Shear stress distribution at the expected point of failure (45 mm from the left side of the specimen in Fig. 13).

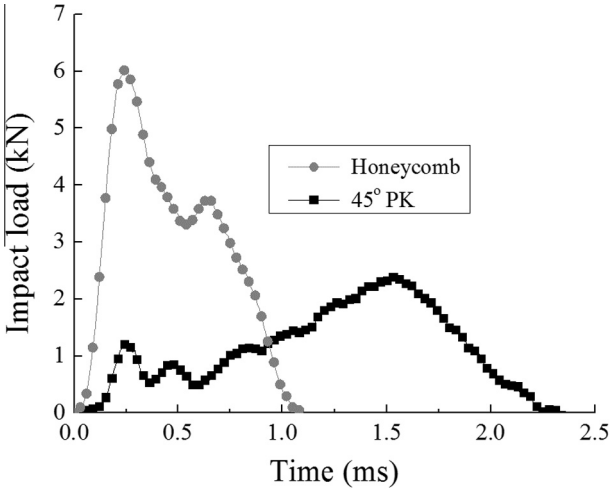

Fig. 16. Load-time curves of impact test with 6 J of impact energy.

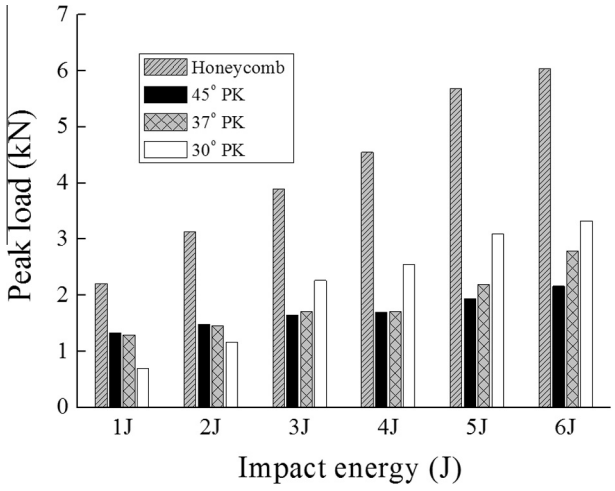

Fig. 15. Peak load with regard to the impact energy.

honeycomb sandwich structure was low because of its structural characteristics. The honeycomb structure was very stiff in the height direction so the impact duration is considerably short. The maximum impact load of honeycomb structure was higher than the PK structure because of its short impact duration. The impact load distributions of the 45° PK sandwich structure and the honeycomb sandwich structure with respect to time when the impact energy was 6 J are shown in Fig. 16. The peak load of honeycomb sandwich structure was 3 times greater than the 45° PK sandwich structure as shown in Fig. 15.

Fig. 16 shows the impact load-time curves of the 45° PK sandwich structure and the honeycomb sandwich structure when the impact energy was 6 J. The impact duration of the 45° PK sandwich structure was 2.1 times longer than the honeycomb sandwich structure. The four struts in the PK structure functioned as elastic springs which resulted in the longer impact duration. However, the compression deformation of honeycomb sandwich structure was limited because of its vertically aligned structure and the impact duration was very short even when 6 J of impact energy was applied. From these results, the PK sandwich structure was very efficient for impact load reduction. The most effective sandwich structure for impact load reduction in this research was found to be the 45° PK sandwich structure.

The 45° PK sandwich structure was the best strcture compared to conventional honeycomb sandwich structure and other PK sandwich structures. The maximum specific bending load of the 45° PK sandwich structure was 31% higher than that of the honeycomb sandwich structure and the bending deflection was also 8.3 times higher than that of the honeycomb sandwich structure. In terms of dynamic test, The maximum impact load of 45° PK sandwich structure was 67% lower than the maximum impact load of honeycomb sandwich structure and this means that the 45° PK sandwich structure can efficiently reduce the impact load of impactor than the honeycomb sandwich structure. From the results, the 45° PK sandwich structure was considered to be recommendable sandwich structure from the view point of static and dynamic charateristics.

5. Conclusion

A pyramidal kagome (PK) sandwich structure made of polypropylene material and its manufacturing processes were developed in this research. The PK structure remains the structural advantages of the kagome structure while the fabrication time was considerably reduced because the woven and the brazing process were replaced with the injection molding and the ultrasonic welding process. The mechanical properties of the PK sandwich structure were examined by conducting three-point bending and impact tests. The PK sandwich structure which had 45° core struts angle showed 31% higher maximum specific bending load than the honeycomb sandwich structure. This resulted from the unique adhesive characteristics of the polypropylene material. Furthermore, the PK sandwich structures seem to be more efficient than the honeycomb structure in the impact load reduction aspect because of its struts which was acting as the elastic spring. When the 6 J of impact energy was applied, the maximum impact load of 45° PK structure was 65% lower than the maximum impact load honeycomb sandwich structure. The 45° PK sandwich structure seems to be an effective structure from the view point of both static and dynamic characteristics.

Acknowledgements

This research was supported by the Kolon Plastics, Climate Change Research Hub of KAIST (Grant No. N01150036) and KAIST Institute Research Fund (Grant Nos. N10150022, N10150023).

References

[1] Xiong J, Ma L, Stocchi A, Yang JS, Wu LZ, Pan SD. Bending response of carbon fiber composite sandwich beams with three dimensional honeycomb cores. Compos Struct 2014;108:234–42.

[2] Du YC, Yan N, Kortschot MT. An experimental study of creep behavior of lightweight natural fiber-reinforced polymer composite/honeycomb core sandwich panels. Compos Struct 2013;106:160–6.

[3] Zhang G, Ma L, Wang B, Wu L. Mechanical behaviour of CFRP sandwich structures with tetrahedral lattice truss cores. Compos B Eng 2012;43(2):471–6.

[4] Lu TJ, Valdevit L, Evans AG. Active cooling by metallic sandwich structures with periodic cores. Prog Mater Sci 2005;50(7):789–815.

[5] Wadley HNG, Fleck NA, Evans AG. Fabrication and structural performance of periodic cellular metal sandwich structures. Compos Sci Technol 2003;63(16):2331–43.

[6] Kohrs T, Petersson BAT. Wave propagation in light weight profiles with truss-like cores: wavenumber content, forced response and influence of periodicity perturbations. J Sound Vib 2007;304(3–5):691–721.

[7] Xiong J, Ghosh R, Ma L, Ebrahimi H, Hamouda AMS, Vaziri A, et al. Bending behavior of lightweight sandwich-walled shells with pyramidal truss cores. Compos Struct 2014;116:793–804.

[8] Dragoni E. Optimal mechanical design of tetrahedral truss cores for sandwich constructions. J Sandwich Struct Mater 2013;15(4):464–84.

[9] Yungwirth CJ, Wadley HNG, O'Connor JH, Zakraysek AJ, Deshpande VS. Impact response of sandwich plates with a pyramidal lattice core. Int J Impact Eng 2008;35(8):920–36.

[10] Chen K, Neugebauer A, Goutierre T, Tang A, Glicksman L, Gibson LJ. Mechanical and thermal performance of aerogel-filled sandwich panels for building insulation. Energy Build 2014;76:336–46.

[11] Lou J, Ma L, Wu LZ. Free vibration analysis of simply supported sandwich beams with lattice truss core. Mater Sci Eng B Adv Funct Solid State Mater 2012;177(19):1712–6.

[12] Chiras S, Mumm DR, Evans AG, Wicks N, Hutchinson JW, Dharmasena K, et al. The structural performance of near-optimized truss core panels. Int J Solids Struct 2002;39(15):4093–115.

[13] Kooistra GW, Queheillalt DT, Wadley HNG. Shear behavior of aluminum lattice truss sandwich panel structures. Mater Sci Eng A Struct Mater Prop Microstruct Process 2008;472(1–2):242–50.

[14] Queheillalt DT, Wadley HNG. Pyramidal lattice truss structures with hollow trusses. Mater Sci Eng A Struct Mater Prop Microstruct Process 2005;397(1–2):132–7.

[15] Xiong J, Vaziri A, Ma L, Papadopoulos J, Wu L. Compression and impact testing of two-layer composite pyramidal-core sandwich panels. Composite Structures 2012;94(2):793–801.

[16] Kang K-J. A wire-woven cellular metal of ultrahigh strength. Acta Mater 2009;57(6):1865–74.

[17] Lee BK, Kang KJ. A parametric study on compressive characteristics of Wire-woven bulk kagome truss cores. Compos Struct 2010;92(2):445–53.

[18] Malcom AJ, Aronson MT, Deshpande VS, Wadley HNG. Compressive response of glass fiber composite sandwich structures. Compos A Appl Sci Manuf 2013;54:88–97.

[19] George T, Deshpande VS, Sharp K, Wadley HNG. Hybrid core carbon fiber composite sandwich panels: Fabrication and mechanical response. Compos Struct 2014;108:696–710.

[20] Xiong J, Ma L, Vaziri A, Yang J, Wu L. Mechanical behavior of carbon fiber composite lattice core sandwich panels fabricated by laser cutting. Acta Mater 2012;60(13–14):5322–34.

[21] Xiong J, Wang B, Ma L, Papadopoulos J, Vaziri A, Wu L. Three-dimensional composite lattice structures fabricated by electrical discharge machining. Exp Mech 2014;54(3):405–12.

[22] Jacobsen AJ, Barvosa-Carter W, Nutt S. Compression behavior of micro-scale truss structures formed from self-propagating polymer waveguides. Acta Mater 2007;55(20):6724–33.

[23] Yin S, Wu L, Ma L, Nutt S. Pyramidal lattice sandwich structures with hollow composite trusses. Compos Struct 2011;93(12):3104–11.

[24] Griskevicius P, Zeleniakiene D, Leisis V, Ostrowski M. Experimental and Numerical Study of Impact Energy Absorption of Safety Important Honeycomb Core Sandwich Structures. Mater Sci Medziagotyra 2010;16(2):119–23.

[25] Tan CY, Akil HM. Impact response of fiber metal laminate sandwich composite structure with polypropylene honeycomb core. Compos B Eng 2012;43(3):1433–8.

[26] Fan HL, Fang DN, Jing FN. Yield surfaces and micro-failure mechanism of block lattice truss materials. Mater Des 2008;29(10):2038–42.

[27] Lee YH, Lee BK, Jeon I, Kang KJ. Wire-woven bulk Kagome truss cores. Acta Mater 2007;55(18):6084–94.

[28] Suzer S, Argun A, Vatansever O, Aral O. XPS and water contact angle measurements on aged and corona-treated PP. J Appl Polym Sci 1999;74(7):1846–50.

[29] Lee D, Kim KH, Choi I, Lee DG. Dynamic properties of the corrugated stainless steel membrane reinforced with the glass composite pressure resisting structure for LNG carriers. Compos Struct 2014;107:382–8.